12R.5 WATER VAPOR AND LIQUID WATER ESTIMATES USING SIMULTANEOUS S AND KA BAND RADAR MEASUREMENTS

Scott Ellis[1], J. Vivekanandan[1], K. Goodman, Jr[2]. and C. Kessinger[1]

1. NCAR, Boulder, CO
2. Norfolk State University

1. Introduction

Using simultaneous S and Ka band observations it is possible to retrieve a path integrated value of the water vapor content as well as cloud liquid water content values using the atmospheric and liquid water attenuation properties at the two frequencies. Recently the NCAR S-band dual polarimetric (S-Pol) radar has been upgraded to include simultaneous Ka-band radar measurements (Farquharson et al, 2005). The Ka band antenna is mounted on the side of the S-band antenna and the two radars have matched beam widths and range resolutions.

Atmospheric, or gaseous, attenuation at radio frequencies is mainly due to absorption by water vapor molecules with a small contribution by molecular oxygen. The attenuation depends on the concentrations of the absorbing gases, temperature and pressure. The attenuation due to oxygen is predictable and can be accounted for because molecular is oxygen evenly distributed in the troposphere. The temperature dependence, which is weak, and pressure dependence are accurately accounted for by layer based radiative transfer models (Liebe 1985). Thus, in principle, it is possible to estimate a path integrated value of water vapor content from accurate atmospheric attenuation estimates.

The atmospheric attenuation at S-band (10 cm wavelength) is negligible in comparison to the Ka-band (8 mm). In the absence of propagation effects, the reflectivity of cloud echoes measured by the S and Ka-band radars should be equivalent, provided the Rayleigh scattering approximation is satisfied for both wavelengths. If there are no intervening echoes, accurate approximations of two way atmospheric attenuation can be obtained by subtracting Ka-band reflectivity from S-band reflectivity at the edges of the cloud nearest to the radars. This estimate is then used to approximate the path integrated water vapor content.

The data used in the current study was obtained from the Rain In Cumulus over the Ocean (RICO) experiment conducted in December and January 2004/2005 in the Caribbean Sea. This data set is ideal because there were numerous trade wind cumulus clouds providing different radar paths for the retrieval. Further, there were dropsondes and upsondes in close proximity for comparison.

The liquid water attenuation through clouds can also be estimated by comparing S and Ka-band reflectivity and used to infer cloud water content values. Details can be found in Vivekanandan et al (1999) and will not be shown in this paper. Results of the liquid water retrieval will be presented at the conference.

2. Water Vapor Retrieval Method

The proposed method for retrieval of water vapor from dual wavelength radar observations includes three steps: 1. Selection of appropriate data, 2. Estimation of Ka-band atmospheric attenuation, and 3. Retrieval of humidity using a radiative transfer model.

2.1 Data Selection

There are a number of criteria that have been developed to ensure the data used in the water vapor retrieval is appropriate. A small patch of data is selected, currently by hand, at the edges of weather echoes nearest the radar in order to avoid contamination by liquid water attenuation. Liquid attenuation at Ka-band is much stronger than gaseous absorption. Therefore data were not collected more than 0.5 km

Corresponding author address: Scott Ellis, NCAR P.O. Box 3000, Boulder, CO 80307-3000

into any weather echo. Currently data with any intervening weather echoes must be avoided. In the future, however, liquid water attenuation could be accounted for, thereby relieving the procedure from this restriction. The data patches contain from 10 to 30 radar range gates.

The power returned from Bragg scatter can be strong at S-band, and is generally much smaller at Ka-band. Data must be selected that is not significantly affected by the Bragg scatter power associated with the turbulence at the edges of clouds. The edges of the liquid cloud echo can be roughly determined by the Ka-band reflectivity. The selected data must have S-band reflectivity values at least 5 dBZ above the observed Bragg scatter echoes surrounding the liquid cloud.

The selected data must satisfy the Rayleigh scattering approximation for both radar wavelengths. Drop diameters of less than roughly 1 mm satisfy this condition. Only data with average differential reflectivity (ZDR) values less than 0.25 dB and reflectivity (Z) less than 20 dBZ are allowed. Further the median dropsize diameter, D_0, is estimated from Z and ZDR. If the mean D_0 exceeds 0.5 mm the data are rejected.

Also the effects of partial beam blockage and point targets such as birds must be avoided. To help identify any problems a point by point correlation coefficient between S- and Ka-band reflectivity values over each data patch is computed. Data with less than 0.7 correlation are rejected.

2.2 Attenuation Estimation

The difference between S-band and Ka band reflectivity in the absence of absorption by liquid water, violation of the Rayleigh approximation and contamination by radar Bragg scatter and other radar artifacts, can be used to obtain an accurate estimate of the atmospheric attenuation along the radial.

Once suitable data have been selected the average S- and Ka-band reflectivity values and average range are computed. The averages of reflectivity are computed in linear units. The two-way gaseous attenuation (dB km^{-1}) is estimated simply as the difference of mean S-band dBZ and mean Ka band dBZ values divided by range.

2.3 Humidity Estimation

With the atmospheric attenuation estimation along a radial, it is possible infer the path integrated water vapor content using a full radiative transfer model. The model used in this study is from Liebe (Liebe, 1985) and computes the attenuation due to water vapor and molecular oxygen absorption over propagation paths through atmospheric layers defined by their depth as well as pressure and temperature at the bottom and top of the layers.

The model was run numerous times over the range of temperatures and pressures found in RICO over the boundary layer. Figure 1 shows a scatter plot of the model computed specific humidity (g m^{-3}) versus one-way atmospheric attenuation (dB km^{-1}). The tight scatter indicates that the temperature and pressure dependence over the range of values in question are small. Both second and third degree polynomial fits were computed and are plotted in Figure 1 as the blue solid line and red solid line, respectively. The third degree polynomial fit was chosen for the retrieval algorithm and yielded the following equation for specific humidity (SH, in g m^{-3}),

$$SH = 201.40a^3 - 209.60a^2 + 120.55a - 2.25,$$

where a is the one-way atmospheric attenuation.

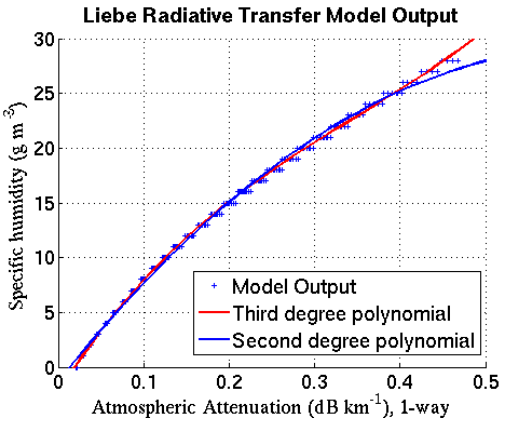

Figure1. Scatter plot of specific humidity (g m-3) versus one-way attenuation (dB km^{-1}), overlaid with second (blue solid line) and third (red solid line) polynomial fit curves.

2.4 Errors From Radar Calibration

The accuracy of the attenuation approximation depends on the consistency of both radar calibrations and the range from radar. An analysis of the errors in attenuation estimation due to radar calibration as a function of range was performed to determine the minimum acceptable range for application of the method. Figure 2 shows the error as a function of range resulting from errors in the reflectivity difference of 0.5 (red) and 1.0 dB (blue) for a) gaseous attenuation, and b) the resulting error in specific humidity. The error decreases with increasing range. If 1 g m^{-3} error is acceptable than the minimum range is about 15 km (30 km) for 0.5 dB (1.0 dB) error in reflectivity difference.

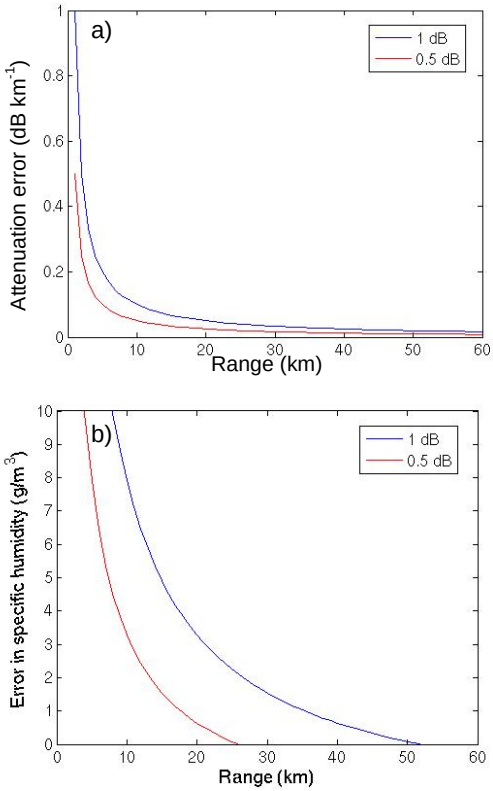

Figure 2. Plots of error as a function of range resulting from errors in the reflectivity difference of 0.5 (red) and 1.0 dB (blue) for a) gaseous attenuation, and b) specific humidity

3. Results

The initial analysis using data from the Rain In Cumulus over the Ocean (RICO) experiment shows encouraging results. Figure 3 shows a comparison of the radar retrieved water vapor estimates (red points, g m^{-3}) and water vapor measured by two proximity dropsondes (solid lines) from the NCAR C-130 aircraft. The data was collected on January 11 2005, and the dropsondes are approximately 5 minutes apart and 40 minutes from the radar retrieval time. The elevation of the midpoints of the radar paths are used to plot the retrieved, radar path integrated, specific humidity.

It can be seen that the radar retrieved humidity profile is in agreement with the dropsonde values to within roughly 1 g m^{-3}, or about 5%, and that the trend of drying with height is captured. The values with the largest errors come from the shortest paths, as predicted. The shortest path length is roughly 15 km and the errors are around 1 g m^{-3}, suggesting the difference in S and Ka-band reflectivity are accurate to within about 0.5 dB.

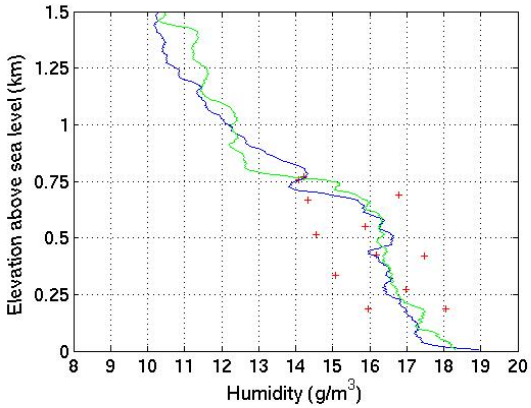

Figure 3. Plots of radar retrieved (red points) and dropsonde measured (solid lines) specific humidity (g m^{-3}).

4. Summary and Conclusions

The NCAR S-Pol radar has been upgraded to include simultaneous Ka-band radar measurements with resolution volumes matched to the S-band radar, providing a unique dual wavelength platform. This instrument provides an opportunity to retrieve more information about the state of clouds and the atmosphere then previously possible with weather radar, including liquid water content and water vapor content. The initial results of path integrated values of water vapor

content show good agreement with in-situ sounding measurements.

5. Acknowledgements

Portions of this work were sponsored by the National Science Foundation. The views expressed in the paper are those of the authors and do not necessarily represent the official policy position of the U.S. government.

6. References

Farquharson, G., F. Pratte, M. Pipersky, D. Ferraro, A. Phinney, E. Loew, R. A. Rillng, S. M. Ellis, and J. Vivekanandan, 2005: NCAR S-Pol Second Frequency (Ka-band) Radar. *32nd Conf. on Radar Meteor. AMS*, Albuquerque, N.M.

Liebe, H. J., 1985: An updated model for millimeter wave propagation in moist air. *Radio Sci*., **20**, 1069 – 1089

Vivekanandan, J., B. Martner, M.K. Politovich and G. Zhang, 1999: Retrieval of atmospheric liquid and ice characteristics using dual-wavelength radar observations. *IEEE Trans. On Geoscience and Remote Sensing,* 37, 2325-2334.